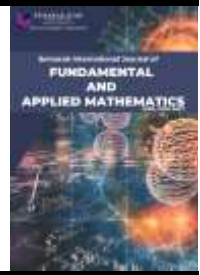




## Semarak International Journal of Fundamental and Applied Mathematics

Journal homepage:  
<https://semarakilmu.my/index.php/sijfam>  
ISSN: 3030-5527



# Numerical Investigation of Non-Newtonian Williamson Hybrid Ferrofluid Flow over a Stretching Sheet: Effects of Magnetic, Stretching and Thermal Parameters

Puteri Ereena Shafira Mustafa<sup>1</sup>, Syazwani Mohd Zokri<sup>1,\*</sup>, Nur Syamilah Arifin<sup>2</sup>, Siti Farah Haryatie Mohd Kanafiah<sup>3</sup>, Abdul Rahman Mohd Kasim<sup>4</sup>, Hussein Ali Mohammed Al-Sharifi<sup>5</sup>

- <sup>1</sup> College of Computing, Informatics and Mathematics, Universiti Teknologi MARA (UiTM) Terengganu Branch, Kuala Terengganu Campus, 21080 Kuala Terengganu, Malaysia  
<sup>2</sup> College of Computing, Informatics and Mathematics, Universiti Teknologi MARA Cawangan Johor Kampus Pasir Gudang, 81750, Masai Johor, Malaysia  
<sup>3</sup> Mathematical Sciences Studies, College of Computing, Informatics and Mathematics, Universiti Teknologi MARA (UiTM) Kelantan Branch, Machang Campus, 18500, Malaysia  
<sup>4</sup> Centre for Mathematical Sciences, Universiti Malaysia Pahang Al-Sultan Abdullah, Gambang, 26300 Kuantan, Pahang, Malaysia  
<sup>5</sup> Department of Mathematics, College of Education for Pure Sciences, University of Kerbala, Karbala, 1125, Iraq

### ARTICLE INFO

### ABSTRACT

#### Article history:

Received 15 December 2024  
Received in revised form 21 January 2025  
Accepted 22 February 2025  
Available online 15 March 2025

#### Keywords:

Williamson fluid; hybrid ferrofluid;  
stretching sheet; heat transfer

Non-Newtonian Williamson fluid has become the topic of interest among researchers due to shear thinning properties that can represent real life applications. Hybrid ferrofluid are also considered because of its higher heat transfer rather than a single domain ferrofluid. This research aims to discover the flow of non-Newtonian Williamson hybrid ferrofluid along the stretching sheet. Partial differential equations (PDEs) are transformed into ordinary differential equations (ODEs) by using similarity transform variable. The transformed ODEs are solved numerically by using mathematical algorithm encoded in Maple software. The effect of velocity and temperature profiles are discussed for several parameters such as magnetic parameter, stretching parameter, non-Newtonian Williamson fluid parameter, Prandtl number and local Eckert number. It is discovered that the velocity profile increases as the value of magnetic and stretching parameter are increased. On the other hand, the temperature profile increases due to increasing magnetite and copper nanoparticles volume fraction, stretching parameter, non-Newtonian fluid parameter and Eckert number.

## 1. Introduction

Ferrofluid is a type of fluid that is controlled by magnetic field. It is also known that ferrofluid is a stable colloidal suspension following an ultrafine single-domain nanoparticles [1]. It consists of a few liquid carriers such as ethylene glycol, water, and oil. Besides, it also embraces of chemical agents

\* Corresponding author.

E-mail address: [syazwanimz@uitm.edu.my](mailto:syazwanimz@uitm.edu.my)

<https://doi.org/10.37934/sijfam.5.1.2534b>

like lactic acid, oleic acid and magnetic nanoparticles like maghemite and magnetite [2,3]. Ferrofluid is also known as a single-domain liquid core with a colloidal interruption of a ferromagnetic element.

Hybrid ferrofluid is the outcome of suspending chemical agents such as magnetite and cobalt ferrite. Hybrid ferrofluid is defined as the ferroparticles that subsist with two different ferrofluid such as 50% of water and 50% ethylene glycol. According to Saranya *et al.*, [4], the merit of using hybrid ferrofluid rather than base fluid or any simple nanofluid is that hybrid ferrofluid has the highest skin friction and heat transfer on a surface. It diminishes the size of ferroparticles, thus allowing the ferromagnetism to change into superparamagnetism. Hybrid ferrofluid has been used widely for various industries up to this date. In the bio-medical industry, this fluid has been actively used in magnetic resonance and particle imaging.

Magneto-hydrodynamic stagnation point flow has been studied and introduced as the heat transfer for various temperatures of plates. The history of the stagnation point flow on the stretching sheet started when Crane [5] analysed the flow on a stretching plate and use the Navier-Stoke's equation to acquire the analytical solution. Then Gupta and Gupta [6] followed Crane's steps by adding the element of mass transferring effect to the study. The study of heat transfer mechanism has gained researchers interest due to numerous industrial applications such as plastic-molding, manufacturing of fiber-glass, and enhancement in paint [7]. Uddin *et al.*, [8] also learned that stagnation point flow happened on various types of geometry.

In this study, the non-Newtonian Williamson and ferrofluid have been taken into consideration. Blood has been considered as one of Williamson fluids. Williamson fluid which has a characteristic of shear thinning also known as pseudoplastic fluid. According to past research, blood is also classified as an electrically conductive liquid [9]. Since pseudoplastic fluid would not be following the Newton condition, it has been transcribed that the flow process of Williamson fluid will be inclined to follow the horizontal locus. Thus, the Runge-Kutta Fehlberg method has been used to solve the problem numerically [10].

There are many studies that have been conducted on hybrid ferrofluid to beneficiate the growth of engineering applications. Yahya *et al.*, [11] studied the effect of thermal dissipation, heat source, and invariant magnetic field within the bulk engine oil containing Molybdenum disulphide ( $MoS_2$ ) and Zinc oxide ( $ZnO$ ) when the oil is poured over a stretching sheet. There is a significant increase in the effectiveness of thermal conductivity when it came to hybrid nanofluid. The nanostructure of the hybrid nanofluid allows them to be more heat generative than the mono nanofluid [12]. Neethu *et al.*, [13] studied the radiation flow on an exponentially stretching sheet. Authors recorded that the incremented radiation escalated on exponentially stretching sheet and diminished on the surface of an exponentially shrinking sheet.

There are many studies on Williamson fluid that relates with engineering and biological field. Hayat *et al.*, [14] discovered that there is a difference between the stagnation flow of magneto Williamson on different thickness of the stretching sheets. The study of the homogeneous-heterogeneous reaction on Williamson fluid over a stretchable sheet has been done by Hussain *et al.*, [10]. The impact of bioconvection aspects such as nonlinear thermal radiation, sink effect, heat source, and chemical reaction in Williamson fluid over a stretching sheet has been discussed by Awan *et al.*, [15]. Some of the medical features involved are chemical reactions, magnetic dipole, and activation energy. The impact of Williamson nanofluid over a wide range of the physical parameter, temperature, and also thermal relaxation also has been counted by Amjad *et al.*, [16]. Ramzan *et al.*, [17] studied the effect of medical features on the MHD flow of non-Newtonian Williamson Ferro-nanofluid on a stretched sheet. Non-Newtonian fluid is known as a time-dependent fluid that affects the shear rate according to the stress given to the fluid [18]. It has been studied that the Brinkmann

ratio bring an effect on specific surface temperature and wall heat flux for non-Newtonian fluid heat and mass transpiration flow on a porous shrinking and stretching sheet [19].

Motivated by the above-mentioned studies, the numerical solution of Williamson hybrid ferrofluid over a stretching sheet is considered in this study. The governing equations of partial differential equations (PDEs) are reduced to ordinary differential equations (ODEs) by applying similarity transformation variables. Fetching the results from the transformation process, the ODEs will be managed in Maple software by using the Runge-Kutta Fehlberg method.

## 2. Methodology

The flow of Williamson fluid over a stretching sheet is considered as shown in Figure 1. Blood has been selected as their based fluid, while small amount of copper will be mixed with magnetite which considered as ferroparticles and served as the non-Newtonian Williamson hybrid ferrofluid.

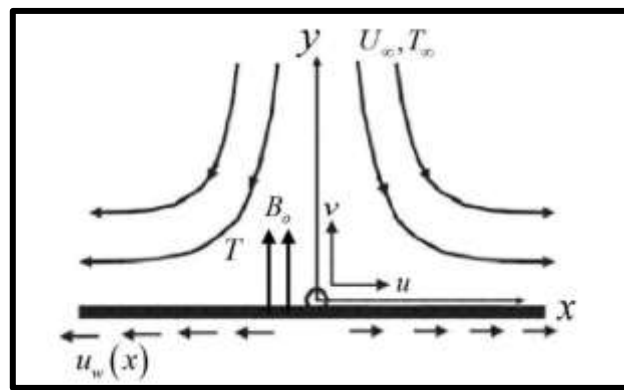


Fig. 1. Figure of flow configuration

Three types of governing equation considered in this research are as the following [20].

$$\frac{\partial u}{\partial x} + \frac{\partial v}{\partial y} = 0 \quad (1)$$

$$u \frac{\partial u}{\partial x} + v \frac{\partial v}{\partial y} = U_{\infty} \frac{\partial U_{\infty}}{\partial x} + V_{hmf} \frac{\partial^2 u}{\partial y^2} + \sqrt{2} V_{hmf} \Gamma \frac{\partial u}{\partial y} \frac{\partial^2 u}{\partial y^2} - \frac{\sigma B_0^2(x)}{\rho_{hmf}} (u - U_{\infty}) \quad (2)$$

$$u \frac{\partial T}{\partial x} + v \frac{\partial T}{\partial y} = \frac{k_{hmf}}{(\rho C_p)_{hmf}} \frac{\partial^2 T}{\partial y^2} + \left[ \left( \frac{\partial u}{\partial y} \right)^2 + \frac{\Gamma}{\sqrt{2}} \left( \frac{\partial u}{\partial y} \right)^3 \right] \quad (3)$$

Eq. (1) until Eq. (3) are subjected towards the boundary conditions

$$\begin{aligned} u = u_w, \quad v = 0, \quad T = T_w \quad \text{at } y = 0, \\ u \rightarrow U_{\infty}, \quad T \rightarrow T_{\infty} \quad \text{as } y \rightarrow \infty \end{aligned} \quad (4)$$

Considered  $u$  and  $v$  represent the velocity component along  $x$  and  $y$  axis respectively.  $T$  represents the temperature inside the boundary layer while  $T_{\infty}$  represents the ambient temperature.  $U_{\infty}$  and  $u_w$  represent the free stream velocity and stretching velocity, respectively.

Accordingly, the density, hybrid ferrofluid kinematic viscosity, and dynamic viscosity denoted as  $\rho_{hnf}$ ,  $\nu_{hnf}$ , and  $\mu_{hnf}$ , while  $k_{hnf}$  and  $(\rho C_p)_{hnf}$  are denoted as the thermal conductivity of Williamson hybrid ferrofluid and the heat capacity of the hybrid ferrofluid.  $B_0$  and  $\sigma$  are denoted as the uniform magnetic field strength and the electric conductivity. There are also other variables below that relating to the nanoparticles and the base fluid which denoted with  $_{bf}$  and  $_{s1,s2}$  subsequently. Noted that  $\phi_1$  and  $\phi_2$  represent the nanoparticles of  $Fe_3O_4$  and  $Cu$  correspondingly.

$$\begin{aligned} V_{hnf} &= \frac{\mu_{hnf}}{\rho_{hnf}}, \quad \rho_{hnf} = (1-\phi_2) \left[ (1-\phi_1) \rho_f + \phi_1 \rho_{s1} \right] + \phi_2 \rho_{s2}, \quad \mu_{hnf} = \frac{\mu_f}{(1-\phi_1)^{2.5} (1-\phi_2)^{2.5}}, \\ (\rho C_p)_{hnf} &= (1-\phi_2) \left[ (1-\phi_1) (\rho C_p)_f + \phi_1 (\rho C_p)_{s1} \right] + \phi_2 (\rho C_p)_{s2}, \\ \frac{k_{hnf}}{k_{bf}} &= \frac{k_{s2} + 2k_{bf} - 2\phi_2 (k_{bf} - k_{s2})}{k_{s2} + 2k_{bf} - \phi_2 (k_{bf} - k_{s2})}, \quad \frac{k_{bf}}{k_f} = \frac{k_{s1} + 2k_f - 2\phi_1 (k_f - k_{s1})}{k_{s1} + 2k_f - \phi_1 (k_f - k_{s1})} \end{aligned} \quad (5)$$

Since Eq. (1) to Eq. (3) are in a complex form of PDEs, the following similarity variables help to simplify the equation into a simpler form:

$$\eta = \left( \frac{b}{\nu_f} \right)^{1/2} y, \quad \psi = (b\nu_f)^{1/2} x f(\eta), \quad \theta(\eta) = \frac{T - T_\infty}{T_w - T_\infty}, \quad (6)$$

where  $\eta$  and  $\theta$  are denoted as non-dimensional variables while  $\psi$  as the function for the stream. The similarity variables for  $u$  and  $v$  are as follows:

$$u = \frac{\partial \psi}{\partial y} = b x f'(\eta), \quad v = -\frac{\partial \psi}{\partial x} = \left[ -(b\nu_f)^{1/2} f(\eta) \right], \quad (7)$$

By using Eq. (6) and Eq. (7), the resulting ordinary differential equation (ODEs) are obtained as follows;

$$\begin{aligned} &\frac{1}{(1-\phi_1)^{2.5} (1-\phi_2)^{2.5} \left[ (1-\phi_2) \left[ (1-\phi_1) + \phi_1 \left( \frac{\rho_{s1}}{\rho_f} \right) \right] + \phi_2 \left( \frac{\rho_{s2}}{\rho_f} \right) \right]} (f''' - \lambda f'' f''') \\ &+ f f'' - f'^2 + 1 - M(f' - 1) = 0 \end{aligned} \quad (8)$$

$$\begin{aligned} &\frac{\frac{k_{hnf}}{k_f} \theta'' + Pr f \theta'}{(1-\phi_2) \left[ (1-\phi_1) + \phi_1 \left( \frac{(\rho C_p)_{s1}}{(\rho C_p)_f} \right) \right] + \phi_2 \left( \frac{(\rho C_p)_{s2}}{(\rho C_p)_f} \right)} + \frac{Ec}{k_f} \left[ f''^2 + \frac{\lambda}{2} f''^3 \right] = 0 \end{aligned} \quad (9)$$

where the magnetic parameter is  $M = \frac{\sigma B_0^2(x)}{b\rho_{lmf}}$ , the non-Newtonian Williamson fluid parameter is

$$\lambda = x\Gamma \sqrt{\frac{2b^3}{v_f}}, \text{ Prandtl number is } Pr = \frac{v_f(\rho C_p)_f}{k_f}, \text{ and local Eckert number is denoted as}$$

$$Ec = \frac{(bx)^2}{(\rho C_p)_f(T_w - T_\infty)}. \text{ The transformed boundary conditions are listed as below:}$$

$$\begin{aligned} f(0) &= 0, \quad f'(0) = \varepsilon, \quad \theta(0) = 1, \\ f'(\eta) &\rightarrow 1, \quad \theta(\eta) \rightarrow 0 \text{ as } y \rightarrow \infty \end{aligned} \tag{10}$$

where  $\varepsilon = \frac{a}{b}$ .

### 3. Results

Maple software is used to solve the acquired ODEs such as Eq. (8) to Eq. (10) including the transformed boundary conditions in Eq. (11) using the RKF45 method. Magnetic parameter, stretching parameter, non-Newtonian Williamson fluid parameter, Prandtl number, and local Eckert number are some of the variables considered as it is affecting the properties of heat transfer and fluid flow. Table 1 shows the thermophysical properties of blood, magnetite, and copper that will be used throughout the study.

**Table 1**  
 The thermophysical properties of blood, magnetite, and copper

Physical Properties	Blood	Magnetite ( $Fe_3O_4$ ), $\phi_1$	Copper (Cu), $\phi_2$
$\rho$ ( $kg/m^3$ )	1053	5180	8933
$C_p$ ( $J/kg \cdot K$ )	3594	670	385
$k$ ( $W/m \cdot K$ )	0.492	9.7	400

The numerical results for  $C_f Re_x^{\frac{1}{2}}$  attained in this research are initially reviewed by comparison with earlier published research by Rosli *et al.*, [20] while considering different values of magnetic parameter,  $M$  and magnetite nanoparticle volume fraction,  $\phi_1$ . According to the tabulated result in Table 2, it can be concluded that this research and the past research have come to a positive agreement. The results show indistinguishable values that support the validation of the current study via RKF45 method.

**Table 2**

Comparison of numerical values for  $C_f \text{Re}_x^{-\frac{1}{2}}$  with different values of  $\phi_1$  and  $M$ , when  $\varepsilon = \phi_2 = \lambda = 0$ , and  $\text{Pr} = 6.2$ .

$\phi_1$	Rosli <i>et al.</i> , [20]				Present result			
	$M = 1$	$M = 2$	$M = 5$	$M = 10$	$M = 1$	$M = 2$	$M = 5$	$M = 10$
0.01	1.638704	1.936603	2.636534	3.505861	1.638704	1.936603	2.636534	3.505861
0.1	2.154733	2.546441	3.466780	4.609858	2.154733	2.546441	3.466780	4.609858
0.2	2.841595	3.358167	4.571881	6.079338	2.841595	3.358167	4.571881	6.079338

Figures 2 and 3 show the velocity and temperature profiles on different values of magnetite nanoparticles volume fraction,  $\phi_1$  when  $\phi_2 = 0.06$ ,  $\text{Pr} = 6.2$ ,  $M = 1$ ,  $\lambda = 0.5$ ,  $\varepsilon = 0.5$ , and  $Ec = 0.2$ . It can be concluded that both the velocity and thermal boundary layer thickness are increased as  $\phi_1$  increases.

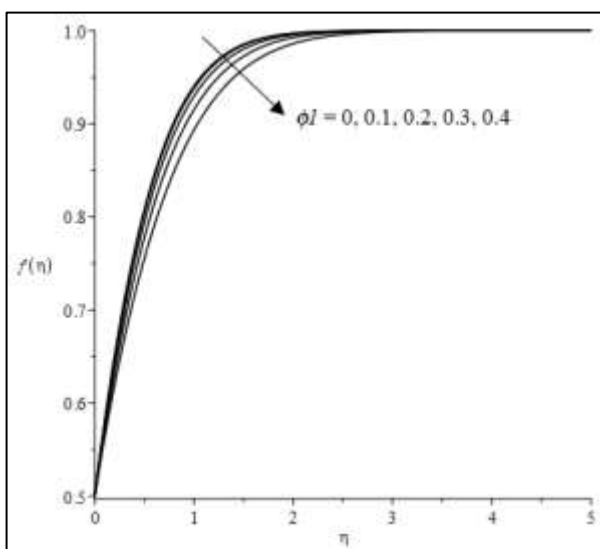


**Fig. 2.** Profile of velocity with different values of magnetite nanoparticles volume fraction

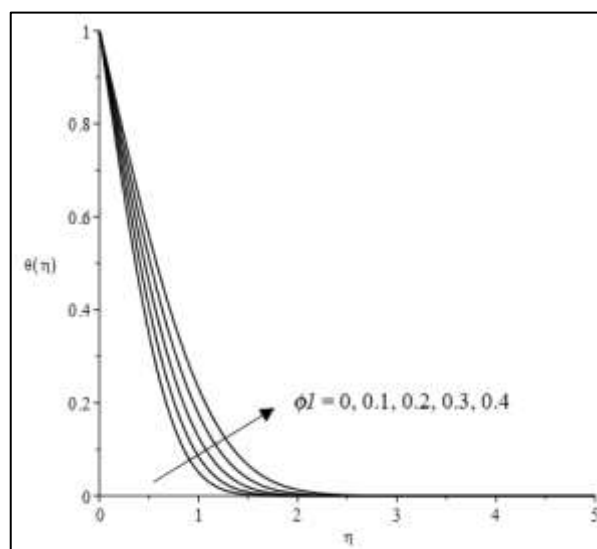


**Fig. 3.** Profile of temperature with different values of magnetite nanoparticles volume fraction

Figures 4 and 5 show the velocity and temperature profiles on different values of nanoparticles volume fraction,  $\phi_1$  when  $\phi_2 = 0.06$ ,  $\text{Pr} = 6.2$ ,  $M = 1$ ,  $\lambda = 0.5$ ,  $\varepsilon = 0.5$ , and  $Ec = 0.2$ . As for the velocity profile, it can be concluded that the velocity boundary layer increases as the parameter value increase. While for the temperature profile, the thermal boundary layer increases following the increase in the values of parameter.

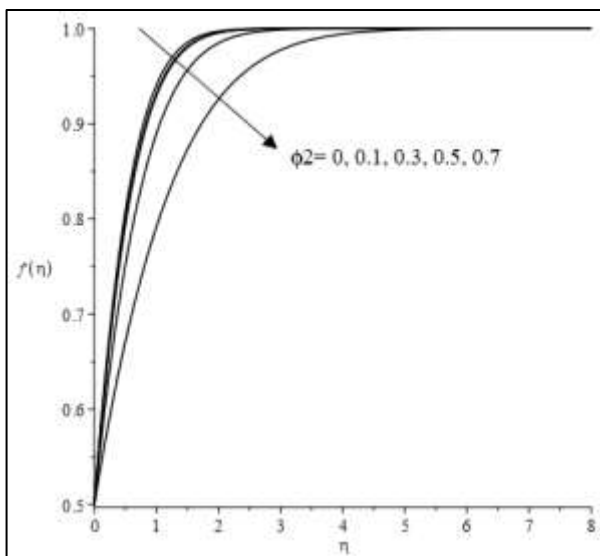


**Fig. 4.** Profile of velocity with different values of copper nanoparticles volume fraction

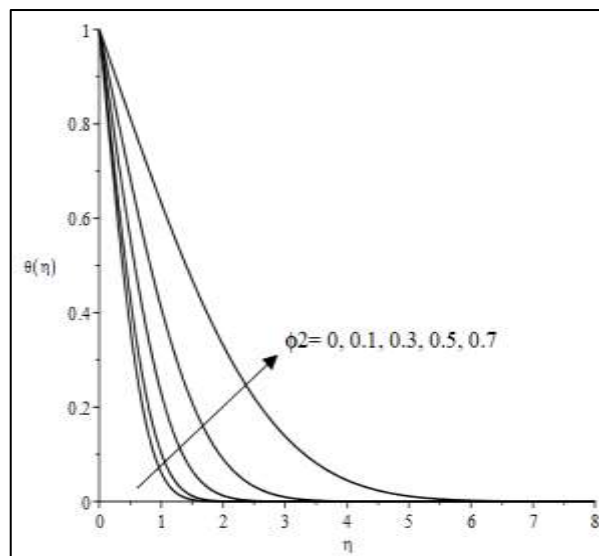


**Fig. 5.** Profile of temperature with different values of copper nanoparticles volume fraction

Figures 6 and 7 portray the reaction of magnetic characteristic by including various values of magnetic parameter,  $M$  towards the profiles for velocity and temperature when  $\phi_1 = 0.1$ ,  $\phi_2 = 0.06$ ,  $Pr = 6.2$ ,  $\lambda = 0.5$ ,  $\varepsilon = 0.5$ , and  $Ec = 0.2$ . It can be highlighted that the velocity profile increases following the increase value of parameter  $M$ . Since ferrofluid also known as a magnetic fluid, the increase in velocity profile shows the significant effect towards the. However, for the temperature profile, the increasing in magnetic parameter resulting towards the diminishing variation of temperature boundary layer. This happen because the nanoparticles in the fluid transform form hot into cold form by following the impact of thermophoresis which acts in the opposite direction as the temperature differential.

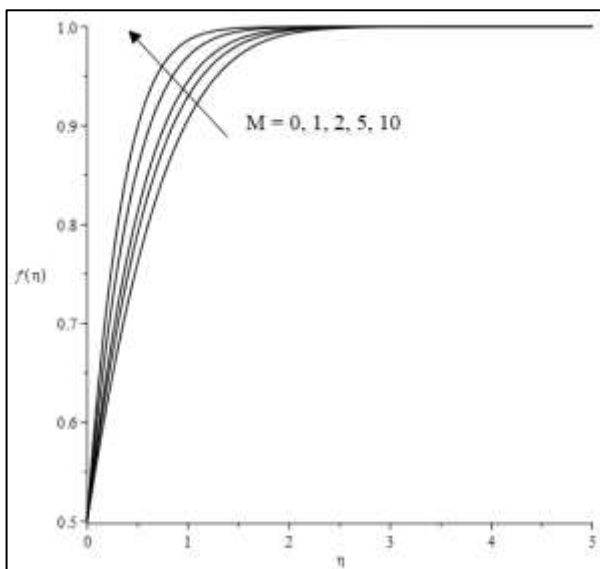


**Fig. 6.** Profile of velocity with different values of magnetic parameter,  $M$

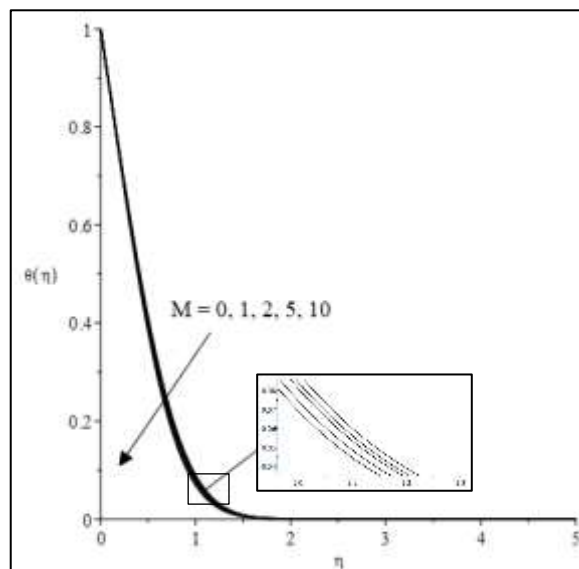


**Fig. 7.** Profile of temperature with different values of magnetic parameter,  $M$

Figures 8 and 9 show the velocity profile and temperature profile following different values of stretching parameter,  $\varepsilon$  when  $\phi_1 = 0.1$ ,  $\phi_2 = 0.06$ ,  $Pr = 21$ ,  $M = 0.5$ ,  $\lambda = 0.1$ , and  $Ec = 0.2$ . Following the velocity profile, it is discovered that the free stream velocity,  $bx$  is greater than the values of stretching velocity of the fluid when the stretching parameter,  $\varepsilon < 1$ . According to Rosli et al., [20], the boundary layer flow becomes transposed and the solidness of the velocity boundary layer decreases when  $\varepsilon > 1$ . On the other hand, the temperature boundary layer thickness increases resulting towards temperature boundary layer decrease in amount as the values of stretching parameter rises.

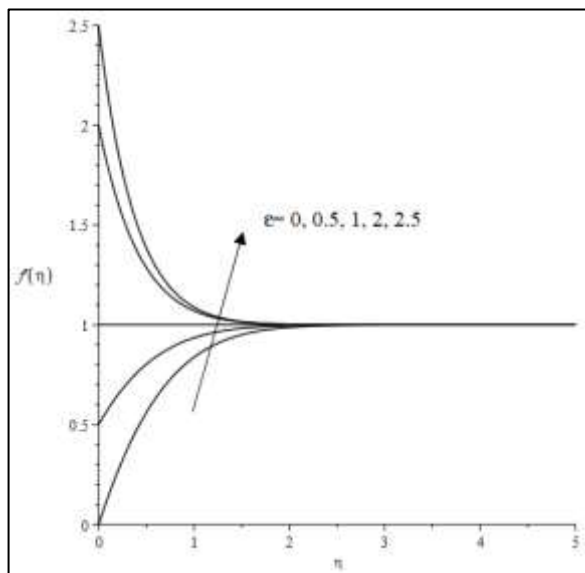


**Fig. 8.** Profile of velocity with different values of stretching parameter,  $\varepsilon$

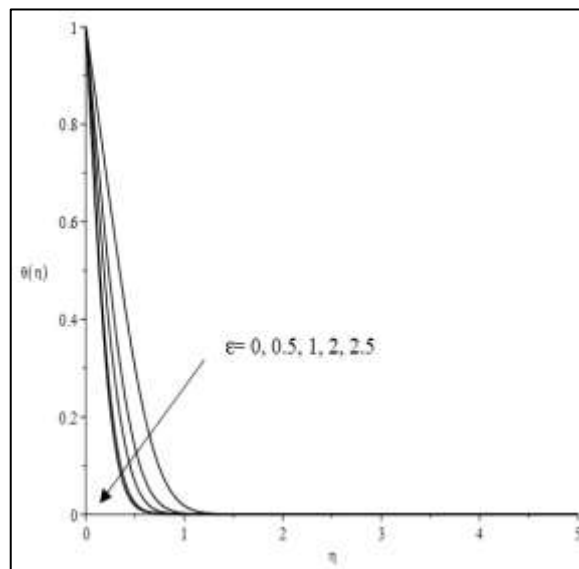


**Fig. 9.** Profile of temperature with different values of stretching parameter,  $\varepsilon$

Figures 10 and 11 illustrate the velocity and temperature profile working on different values of non-Newtonian fluid parameter,  $\lambda$  when  $\phi_1 = 0.1$ ,  $\phi_2 = 0.06$ ,  $Pr = 21$ ,  $M = 0.5$ ,  $\lambda = 0.1$ , and  $Ec = 0.2$ . It has been discovered that the velocity boundary layer thickness increases as the amount of non-Newtonian fluid parameter escalates. This results from the representation of ratio of relaxation towards the time of retardation. As the value of non-Newtonian fluid parameter arise, the time of retardation become diminished as presented in the velocity profile. Meanwhile, the small increment in the temperature boundary layer thickness is observed as the value of non-Newtonian fluid parameter increases. It shows that as the value of parameter increases, it affects the value of ratio of relaxation towards the time of retardation parallelly and resulting in the increases of the temperature boundary layer flow of the fluid.

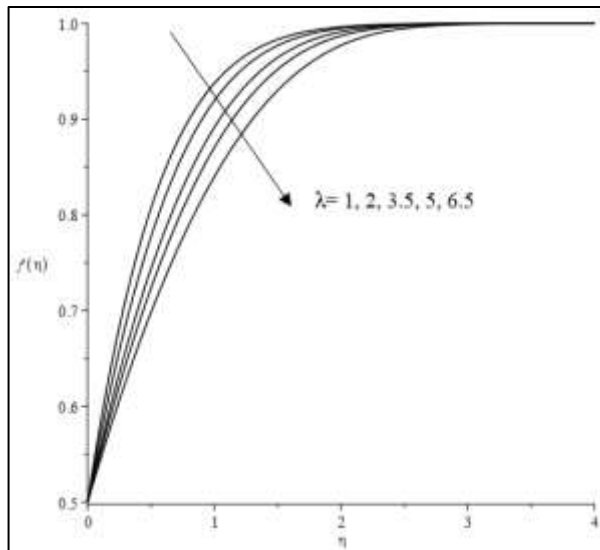


**Fig. 10.** Profile of velocity with different values of non-Newtonian fluid parameter,  $\lambda$

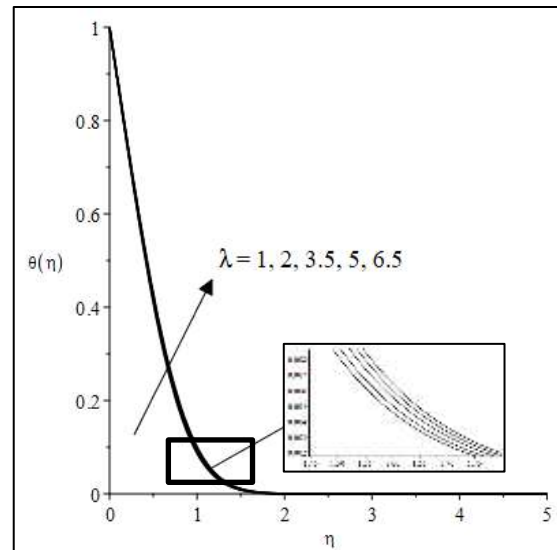


**Fig. 11.** Profile of temperature with different values of non-Newtonian fluid parameter,  $\lambda$

#### 4. Conclusions

It has been verified that the numerical result of  $C_f \text{Re}_x^{\frac{1}{2}}$  achieves a positive agreement with earlier published research by Rosli et al., [20]. For velocity and temperature profile, it has been analysed that there is an increase in magnetite and copper nanoparticles volume fraction for temperature profiles and decreases for velocity profile, respectively. Furthermore, the respective velocity and temperature profile are decreased and increased for non-Newtonian fluid parameter. The temperature profiles of Prandtl number and Eckert number are decreased and increased, respectively whereas the velocity profile exhibits no significant changes due to decoupled boundary layer equation.

#### Acknowledgement

The authors extend their heartfelt gratitude to Universiti Teknologi MARA (UiTM), Terengganu Branch, for their support. Special appreciation is also conveyed to Universiti Teknologi MARA (UiTM), Johor and Kelantan Branches, Universiti Malaysia Pahang Al-Sultan Abdullah, and University of Kerbala, Karbala, Iraq, for their invaluable guidance and contributions.

#### References

- [1] Kole, Madhusree, and Sameer Khandekar. "Engineering applications of ferrofluids: A review." *Journal of Magnetism and Magnetic Materials* 537 (2021): 168222. <https://doi.org/10.1016/j.jmmm.2021.168222>
- [2] Yasin, Siti Hanani Mat, Muhammad Khairul Anuar Mohamed, Zulkhibri Ismail, and Mohd Zuki Salleh. "Magnetite water based ferrofluid flow and convection heat transfer on a vertical flat plate: Mathematical and statistical modelling." *Case Studies in Thermal Engineering* 40 (2022): 102516. <https://doi.org/10.1016/j.csite.2022.102516>
- [3] Arifin, Norihan Md, Rusya Iryanti Yahaya, Ioan Pop, Fadzilah Md Ali, and Siti Suzilliana Putri Mohamed Isa. "Flow and Heat Transfer Analysis of Hybrid Nanofluid over a Rotating Disk with a Uniform Shrinking Rate in the Radial Direction: Dual Solutions." In *International Conference on Computational Heat and Mass Transfer*, pp. 46-55. Cham: Springer Nature Switzerland, 2023.
- [4] Saranya, Shekar, László Baranyi, and Qasem M. Al-Mdallal. "Free convection flow of hybrid ferrofluid past a heated spinning cone." *Thermal Science and Engineering Progress* 32 (2022): 101335. <https://doi.org/10.1016/j.tsep.2022.101335>
- [5] Crane, Lawrence J. "Flow past a stretching plate." *Zeitschrift für angewandte Mathematik und Physik ZAMP* 21 (1970): 645-647. <https://doi.org/10.1007/BF01587695>

- [6] Gupta, P. S., and A. S. Gupta. "Heat and mass transfer on a stretching sheet with suction or blowing." *The Canadian journal of chemical engineering* 55, no. 6 (1977): 744-746. <https://doi.org/10.1002/cjce.5450550619>
- [7] Hamid, Aamir, Masood Khan, and Abdul Hafeez. "Unsteady stagnation-point flow of Williamson fluid generated by stretching/shrinking sheet with Ohmic heating." *International Journal of Heat and Mass Transfer* 126 (2018): 933-940. <https://doi.org/10.1016/j.ijheatmasstransfer.2018.05.076>
- [8] Uddin, Ziya, Korimerla Sai Vishwak, and Souad Harmand. "Numerical duality of MHD stagnation point flow and heat transfer of nanofluid past a shrinking/stretching sheet: Metaheuristic approach." *Chinese Journal of Physics* 73 (2021): 442-461. <https://doi.org/10.1016/j.cjph.2021.07.018>
- [9] Khan, Umair, Aurang Zaib, Anuar Ishak, Sakhinah Abu Bakar, Isaac Lare Animasaun, and Se-Jin Yook. "Insights into the dynamics of blood conveying gold nanoparticles on a curved surface when suction, thermal radiation, and Lorentz force are significant: The case of Non-Newtonian Williamson fluid." *Mathematics and Computers in Simulation* 193 (2022): 250-268. <https://doi.org/10.1016/j.matcom.2021.10.014>
- [10] Hussain, Majid, Shah Jahan, Qasim A. Ranjha, Jawad Ahmad, M. Kashif Jamil, and Akhtar Ali. "Suction/blowing impact on magneto-hydrodynamic mixed convection flow of Williamson fluid through stretching porous wedge with viscous dissipation and internal heat generation/absorption." *Results in Engineering* 16 (2022): 100709. <https://doi.org/10.1016/j.rineng.2022.100709>
- [11] Yahya, Asmat Ullah, Nadeem Salamat, Wen-Hua Huang, Imran Siddique, Sohaib Abdal, and Sajjad Hussain. "Thermal characteristics for the flow of Williamson hybrid nanofluid (MoS<sub>2</sub>+ ZnO) based with engine oil over a stretched sheet." *Case Studies in Thermal Engineering* 26 (2021): 101196. <https://doi.org/10.1016/j.csite.2021.101196>
- [12] Haider, Irfan, Umar Nazir, M. Nawaz, Sayer Obaid Alharbi, and Ilyas Khan. "Numerical thermal study on performance of hybrid nano-Williamson fluid with memory effects using novel heat flux model." *Case Studies in Thermal Engineering* 26 (2021): 101070. <https://doi.org/10.1016/j.csite.2021.101070>
- [13] Neethu, T. S., A. S. Sabu, Alphonsa Mathew, A. Wakif, and Sujesh Areekara. "Multiple linear regression on bioconvective MHD hybrid nanofluid flow past an exponential stretching sheet with radiation and dissipation effects." *International Communications in Heat and Mass Transfer* 135 (2022): 106115. <https://doi.org/10.1016/j.icheatmasstransfer.2022.106115>
- [14] Hayat, Tasawar, Ikram Ullah, Ahmed Alsaedi, and Saleem Asghar. "Flow of magneto Williamson nanofluid towards stretching sheet with variable thickness and double stratification." *Radiation Physics and Chemistry* 152 (2018): 151-157. <https://doi.org/10.1016/j.radphyschem.2018.07.006>
- [15] Awan, Aziz Ullah, Syed Asif Ali Shah, and Bagh Ali. "Bio-convection effects on Williamson nanofluid flow with exponential heat source and motile microorganism over a stretching sheet." *Chinese Journal of Physics* 77 (2022): 2795-2810. <https://doi.org/10.1016/j.cjph.2022.04.002>
- [16] Amjad, Muhammad, Kamran Ahmed, Tanvir Akbar, Taseer Muhammad, Iftikhar Ahmed, and Ali Saleh Alshomrani. "Numerical investigation of double diffusion heat flux model in Williamson nanofluid over an exponentially stretching surface with variable thermal conductivity." *Case Studies in Thermal Engineering* 36 (2022): 102231. <https://doi.org/10.1016/j.csite.2022.102231>
- [17] Ramzan, Muhammad, Sadique Rehman, Muhammad Sheraz Junaid, Anwar Saeed, Poom Kumam, and Wiboonsak Watthayu. "Dynamics of Williamson Ferro-nanofluid due to bioconvection in the portfolio of magnetic dipole and activation energy over a stretching sheet." *International Communications in Heat and Mass Transfer* 137 (2022): 106245. <https://doi.org/10.1016/j.icheatmasstransfer.2022.106245>
- [18] Obalalu, Adebowale Martins, Adebayo Olusegun Ajala, Akintayo Oladimeji Akindele, Olayinka Akeem Oladapo, Olajide Olatunbosun Akintayo, and Oluwatosin Muinat Jimoh. "Computational study of magneto-convective non-Newtonian nanofluid slip flow over a stretching/shrinking sheet embedded in a porous medium." *Computers & Mathematics with Applications* 119 (2022): 319-326. <https://doi.org/10.1016/j.camwa.2022.05.027>
- [19] Mahabaleshwar, U. S., A. B. Vishalakshi, and Martin Ndi Azese. "The role of Brinkmann ratio on non-Newtonian fluid flow due to a porous shrinking/stretching sheet with heat transfer." *European Journal of Mechanics-B/Fluids* 92 (2022): 153-165. <https://doi.org/10.1016/j.euromechflu.2021.12.003>
- [20] Rosli, Wan Muhammad Hilmi Wan, Muhammad Khairul Anuar Mohamed, Norhafizah Md Sarif, Nurul Farahain Mohammad, and Siti Khuzaimah Soid. "Blood conveying ferroparticle flow on a stagnation point over a stretching sheet: non-newtonian williamson hybrid ferrofluid." *Journal of Advanced Research in Fluid Mechanics and Thermal Sciences* 97, no. 2 (2022): 175-185. <https://doi.org/10.37934/arfmts.97.2.175185>